


Article

Mechanical Properties Assessment of Low-Content Capsule-Based Self-Healing Structural Composites

Xenia Tsilimigkra ¹, Dimitrios Bekas ² , Maria Kosarli ², Stavros Tsantzalos ¹,
Alkiviadis Paipetis ² and Vassilis Kostopoulos ^{1,*}

¹ Department of Mechanical Engineering & Aeronautics, University of Patras, Patras University Campus, GR 26500 Patras, Greece; tsilimigkra@upatras.gr (X.T.); tsantzal@mech.upatras.gr (S.T.)

² Department of Materials Science and Engineering, University of Ioannina, 45110 Ioannina, Greece; bekasdim@gmail.com (D.B.); kosarlimaria@gmail.com (M.K.); paipetis@uoi.gr (A.P.)

* Correspondence: kostopoulos@upatras.gr

Received: 31 July 2020; Accepted: 17 August 2020; Published: 19 August 2020



Abstract: Microcapsule-based carbon fiber reinforced composites were manufactured by wet layup, in order to assess their mechanical properties and determine their healing efficiency. Microcapsules at 10%wt. containing bisphenol-A epoxy, encapsulated in a urea formaldehyde (UF) shell, were employed with Scandium (III) Triflate (Sc (OTf)₃) as the catalyst. The investigation was deployed with two main directions. The first monitored changes to the mechanical performance due to the presence of the healing agent within the composite. More precisely, a minor decrease in interlaminar fracture toughness (G_{IIC}) (−14%), flexural strength (−12%) and modulus (−4%) compared to the reference material was reported. The second direction evaluated the healing efficiency. The experimental results showed significant recovery in fracture toughness up to 84% after the healing process, while flexural strength and modulus healing rates reached up to 14% and 23%, respectively. The Acoustic Emission technique was used to support the experimental results by the onsite monitoring.

Keywords: self-healing; capsule based composites; mechanical properties

1. Introduction

Composite materials have been a topic of intense research since their introduction in a variety of engineering fields. However, polymer composites are mostly susceptible to damage during their service. The damage accumulation degrades the mechanical performance of the material and leads often to catastrophic failure [1]. In light of these issues, scientists inspired from biological systems have designed structural materials with a recovery mechanism triggered by the damage itself.

The self-healing functionality can be addressed to a composite material either by incorporating capsules within the polymeric matrix that contains the active healing agent [2], or alternatively by creating vasculature within its structure that deliver the healing agent to the damaged site [3,4], or by employing an intrinsic self-healing polymer as the matrix material [5]. Simultaneously, different integration techniques have been developed according to the selected self-healing system [6].

Focusing more on capsule-based systems, when the capsules are ruptured by a damage event, the self-healing mechanism is triggered through the release of the healing agent. Subsequently, the local healing agent reacts upon contact with the embedded catalyst and restores the desired functionality. Therefore, it is crucial for both components to be present in the damaged area in high quantities, so that the chemical reaction can sufficiently take place [2].

Over the last years, extensive efforts have been made by researchers towards the assessment of the mechanical properties of capsule-based polymer systems. In the majority of the cases that have been studied, the microcapsules are developed by a poly-ureaformaldehyde (pUF) shell, encapsulating

dicyclopentadiene (DCPD) as the liquid healing agent [1,7,8] and/or epoxy resin [9–11]. The chemical mechanism in these systems relies on the ring opening metathesis polymerization (ROMP) of the healing agent and the catalyst. Grubbs' catalyst is well known for its direct catalytic action [12]. However, it is particularly air and moisture sensitive and quite costly. While recognizing the high rate of self-healing efficiency of DCPD and Grubbs' catalyst healing system [7,13], significant drawbacks have been observed regarding the incorporation of these aforementioned system into fiber reinforced polymer (FRP) materials by using conventional manufacturing techniques [14–17]. In view of this, it is of high importance to have efficient compatibility between the commonly used epoxy matrix and the embedded self-healing system. More specifically, Coope et al. [18] developed microcapsules containing a diglycidyl ether bisphenol-A (DGEBA) epoxy monomer encapsulated in a pUF shell as the healing agent and Scandium (III) Triflate ($\text{Sc}(\text{OTf})_3$) as the catalyst. By implementing the self-healing system (20%wt. capsules and 0.5%wt. catalyst) into tapered double cantilever beams (TDCB) the self-healing polymer managed to recover its initial fracture strength at approximately 80%. Furthermore, one more successful attempt to incorporate the healing agent into an epoxy matrix was noted by Rong et al. [19]. In their work, they encapsulated Bisphenol-A (DGEBA) in UF capsules and they integrated them within the matrix material along with an imidazone hardener. The self-healing performance was evaluated in terms of fracture toughness, showing a total recovery of 106% when 20%wt. capsules were added to the matrix. Towards the same direction, Caruso et al. [20] prepared UF microcapsules with a diameter of 200 μm , containing a core solution of 5wt%. epoxy-chlorobenzene [21]. In situ fracture testing with short groove TDCB specimens embedded with 5–20%wt. loadings of the epoxy-containing microcapsules, demonstrated healing efficiencies up to 100%.

The incorporation of microcapsules as a healing system within an FRP material is an attractive recent research area where limited effort has been devoted to the investigation of the self-healing efficiency and also the effects of the integration process regarding the mechanical properties of the final self-healing composite [21]. Capsule-based composite studies are generally focused not only on healing agents, but also on the rupture process, mixing process, micro-structure, and fabrication techniques. As is well known, fiber reinforced materials experience several failure modes during their active lifetime [22]. In more detail, failure mechanisms in a single lamina, include reinforcing fiber failure, matrix cracking, failure of the matrix/fiber interface as well as delamination between individual plies. In a representative study, Manfredi et al. [23] demonstrated that the introduction of 15%wt. of UF capsules within the 'local' matrix of the central ply in a woven glass fiber-reinforced epoxy composite resulted in a decreased interlaminar fracture toughness in Mode I and Mode II at approximately 30% while the peak load decrease reached at 15% and 10%, respectively, as compared to plain composites. Although capsules containing ethyl phenylacetate (EPA) for self-healing purposes did not take place for composite samples due to the presence of bare fibers on the crack plane and to the reduction of EPA diffusion into the matrix. In other work, Yin et al. [24] produced a two-component healing system consisting of UF microcapsules containing epoxy and $\text{CuBr}_2(2\text{-MeIm})_4$ (the complex of CuBr_2 and 2-methylimidazole) as hardener. In the case of 10%wt. of the microcapsules and 2%wt. of the latent hardener, the highest recovery of fracture toughness (GIC) was observed at 68%. Kessler and his co-workers [17] sealed (DCPD) into microcapsules made from UF resin. Then, the microencapsulated monomer (20%wt.) was added into epoxybased composites combined with powdered Grubbs' catalyst. The healing at 80 °C yielded at 80% recovery of the virgin interlaminar fracture toughness in double cantilever beam (DCB) specimens. A two-part healing chemistry was incorporated by Moll et al. [25] in a woven glass/epoxy fiber-reinforced composite. The healing system was comprised of a single type of microcapsules containing silanol end-functionalized polydimethylsiloxane, and a crosslinking agent, polydiethoxysilane, and a second type containing dibutyltin dilaurate catalyst in the solvent hexylacetate. At a concentration of 12 vol.%, a 30% decrease in the short beam strength and at 15 vol.%, a 15% reduction in storage modulus was measured.

Even fewer are the references that study the correlation between the Acoustic Emission (AE) method and the self-healing performance in capsule based FRP composite. On polymeric level,

Szebenyi et al. [26] collected data by detecting the number of hits as a function of displacement and crack propagation and correlated them with the progress of failure during TDCB tests. The accumulation of these hits was significantly higher in the case of the encapsulated material, which can be attributed to capsule fracture phenomena.

Summarizing, the self-healing concepts, especially the capsule-based ones, have been proved as a step-forward towards the development of advanced FRP composites. However, some drawbacks are currently under investigation in order to enable the development of such multifunctional materials. The aim of the current study is to provide new insights in the mechanical and acoustical performance of self-healing fiber reinforced composites integrated with a low content of UF capsules as the self-healing carrier. The healing agent of bisphenol-A/epichlorohydrin (EPON 828) was selected due to its compatibility with the epoxy matrix and the solid-state catalyst of Scandium (III) Triflate (Sc(OTf)₃) due to its increased catalytic ability, low toxicity and high stability [27]. Effort was undertaken to determine the knock down effect in fracture toughness, flexural strength and modulus due to the capsules integration as well as the self-healing efficiency of the developed materials. Focus was given to matrix micro cracking as the main damage mechanism that needs to be healed. For that reason, the experimental results were combined by the onsite use of the nondestructive technique of Acoustic Emission (AE).

2. Materials and Methods

2.1. Materials Selection

The primary materials used for the present study were dry unidirectional carbon fibre (200 g/m²), purchased from TORAY and the matrix material was a two-part epoxy system, supplied by R and G, consisting of an epoxy resin (L) and a hardener (EPH 161). In house Urea Formaldehyde (UF) capsules were synthesized, providing the extrinsic healing functionality. The solvent Ethyl phenylacetate (EPA), the wall materials urea (NH₂CONH₂), the formalin (37%wt. formaldehyde in H₂O), the ethylene maleic anhydride copolymer (EMA, Mw = 100,000–500,000 g/mol), the stabilizers resorcinol (C₆H₄-1,3-(OH)₂), the ammonium chloride (NH₄Cl) and the sodium hydroxide (NaOH) were purchased from Sigma-Aldrich and used as received. The selected healing agent of bisphenol-A/epichlorohydrin (EPON 828) was purchased from Polysciences. Inc. Scandium (III) Triflate (Sc(OTf)₃) with a 99% purity by Sigma-Aldrich was used as the catalyst of the healing agent.

2.2. Microcapsules Synthesis

Although there are several microencapsulation techniques, they are not necessarily appropriate to self-healing application. While the encapsulation method is often suited for specific types of core materials, the emulsification polymerisation method benefits from high strength capsule shell walls, large scale synthesis, thick shell wall and a narrow size distribution. [28]. Therefore, when considering possible commercial exploitation, this is the preferred method for scale-up synthesis. The principle of in situ microencapsulation oil-in-water emulsion polymerisation synthesis, is based on the methodology employed by Brown et al. (2003) [29]. In detail, 2.5 g EMA powder was mixed overnight with 100 mL of deionized water, in a warm bath in order to achieve a 2.5% (*w/v*) aqueous surfactant solution. Before the encapsulation process, the resin was diluted with a non-toxic solvent which was ethyl-phenylacetate EPA, to decrease the viscosity of the healing agent. For the encapsulation process, 100 mL of deionized H₂O was placed in a high shear stirrer (Dispermat D-51580) with 25 mL of 2.5% (*w/v*) EMA aqueous surfactant solution at room temperature. Under continuous agitation 2.5 g urea, 0.25 g ammonium chloride, and 0.25 g resorcinol were dissolved in the solution. After the addition of those chemicals, the pH was adjusted from approximately 2.7 to 3.5 by drop-wise addition of sodium hydroxide (NaOH). Subsequently 60 mL of the core material was then dispersed (epoxy resin—solvent, 15% dilution), in the mixture and the agitation continued at 400 rpm for 10 min. Furthermore, 6.33 g of formalin solution was then added, and the temperature was increased to 55 °C with a rate of 10 °C/min. The chemical

reaction took place for 4 h under continuous agitation with the temperature at 55 °C. Once cooled to ambient temperature, the suspension of microcapsules was recovered by filtration using a Buchner funnel while drying achieved at 25 °C using a laboratory oven.

2.3. Microcapsules Characterization

Microcapsule size analysis and surface morphology characterization were performed using a JEOL JSM 6510LV, Oxford Instruments scanning electron microscope. Microcapsule samples were prepared on glass slides, dried in a vacuum oven, and sputter coated with gold. The accelerating voltage for the Scanning Electrode Microscopy (SEM) measurements was selected at 5.0 kV.

2.4. Composites Manufacturing

Composite plates intended for three points bending and Mode II experiments were manufactured according to ASTM D7264/D6264M-07 and AITM 1.0006, respectively. The selected manufacturing method was wet layup for all the 12 layers. The wet layup technique was selected as composites are developed with lower values of fiber volume fraction (vf). The matrix domination with regards to the fibers intensify the polymerization process once capsules are activated.

UF capsules were implemented in polymers, as previous in house work, at two different contents 5 and 10%wt. following the literature review as stated in the introduction section. The combination of 10%wt. UF capsules with 2.5%wt. scandium triflate exhibited the most promising results in terms of knock down effect and healing efficiency. For that reason, those contents were selected for further implementation within FRPs.

The self-healing efficiency of a capsule-based system is dependent strongly on the dispersion of the capsules into the epoxy material. In view of this, 10%wt. capsules were incorporated into the epoxy modified resin and manual mixing was performed until the mixture was homogeneous. Subsequently, the hardener of the epoxy was added. Due to the high activity of the scandium triflate, it was incorporated right before the fabric impregnation, at a content of 2.5%wt. The final mixture was placed in a vacuum chamber for degassing in order to eliminate air inclusion during mixing process.

The fabric impregnation followed layer by layer. The matrix material containing the self-healing agents (Figure 1a) was impregnated at the lower (3rd and 5th) and upper (9th and 11th) layers to avoid the neutral mid layer at three-point bending loading conditions. In the case of Mode II tests the mid layer was the area of interest and therefore capsule-modified matrix material (Figure 1a) was used for the carbon fabric impregnation, while the neat matrix material (Figure 1b) impregnated the remaining layers. A 13 µm thick PTFE film was also placed in the middle plane of Mode II composite plate to generate the starter crack, which is required according to AITM 1.0006. Figure 2 depicts the schematic of the reference and the modified mid plane.T

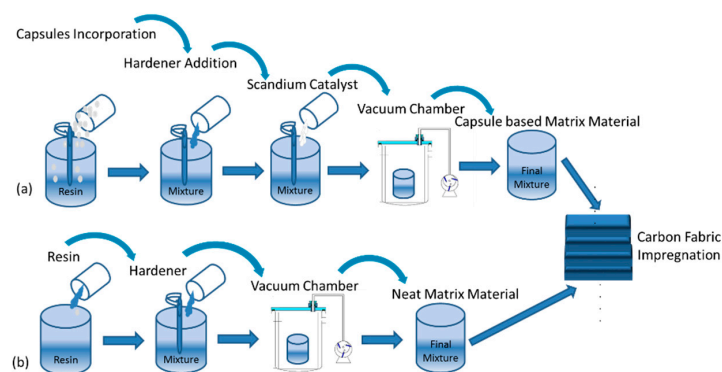


Figure 1. (a) Mixing process of the capsule modified matrix material for the manually impregnation of the composite through wet layup technique. (b) Mixing process of the neat matrix material for the manually impregnation of the composite through wet layup technique.

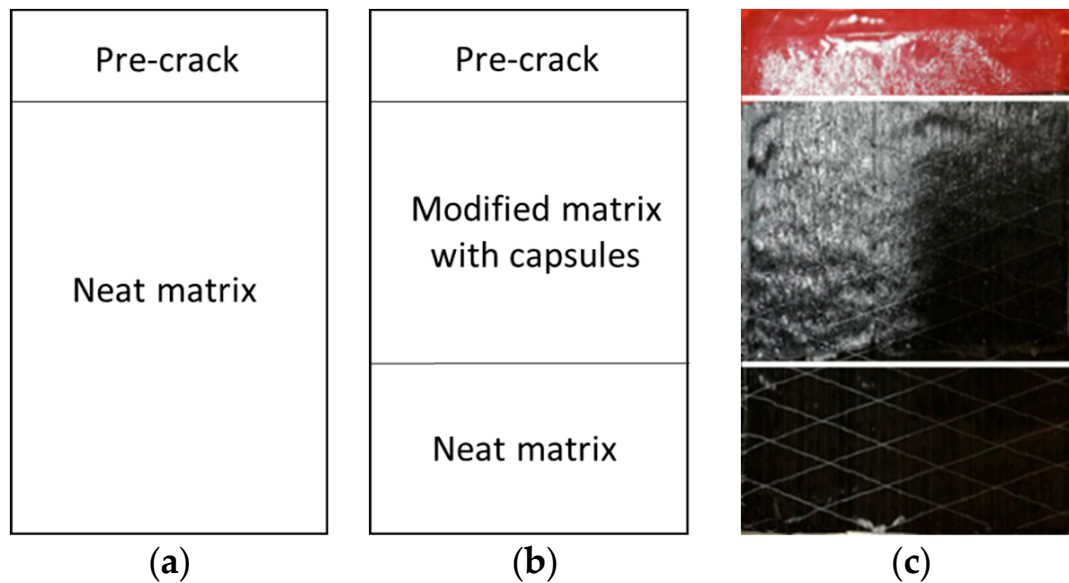


Figure 2. Schematic representation of the (a) reference and (b) modified Mode II mid plane. (c) Mode II modified mid plane during manufacturing.

The consumables that have been also employed for the wet layup process were the peel ply at the top of the laminate to provide a smooth surface to the composite, the perforated release film which allows the removal of the excess resin, the breather to absorb the excess resin.

Curing was undertaken according to the manufacturer's recommendations at room temperature for 24 h and 15 h at 60 °C in a program-controlled oven. The fiber volume fraction was calculated at 40%.

The mechanical properties of the aforementioned modified composites were compared with those of the reference (no healing functionality).

2.5. Quality Control

Ultrasonic C-Scan technique was employed for the quality control of the manufactured composite plates. The equipment consists of a MISTRAS Group AD-IPR 1210-PCI card and a VUB2000 tank. The transducer was a Krautkramer single element probe at 5 MHz, non-focal.

The color bar presents the signal response from the weakest (green), at areas where damage occurs, to the strongest (red) which indicate no major defects within the material. The reference composite plates are depicted in Figure 3a1,a2 for both 3-Point Bending (3PB) and Mode II. Comparing the modified to the reference composites, it is obvious that the reference material has slightly better quality as capsules act as inherent voids within the material. Overall, the quality of the produced composites was considered acceptable in order to continue the experimental campaign.

2.6. Fracture and Bending Experiments

The Mode II interlaminar fracture toughness, G_{IIC} , was measured using the three-point end-notched flexure (3ENF) method in accordance with Airbus Standard, AITM 1.0006 on a hydraulic universal testing machine of 25 kN (Instron 8872) at room temperature conditions (Figure 4b).

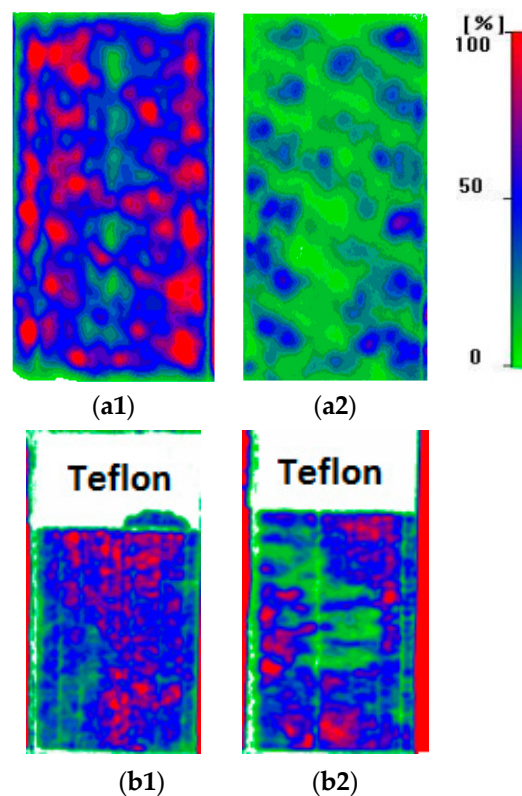


Figure 3. Reference composites for (a1) 3PB and (b1) Mode II and the respective modified (a2,b2).

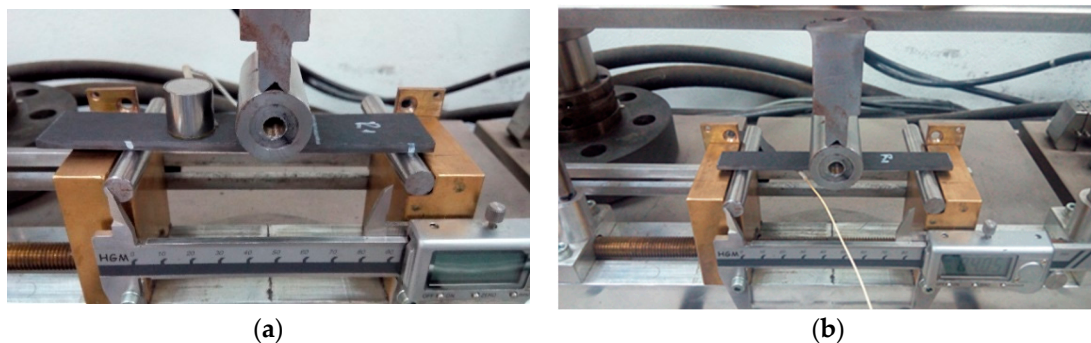


Figure 4. Mode II (a) and three-point bending (b) experiments.

The flexural stiffness and the strength properties of polymer matrix composites were determined by the three-point bending loading system according to ASTM D7264/D6264M-07 (Figure 4b) at the same testing machine.

2.6.1. On Site Monitoring through Acoustic Emission Technique

An AE sensor was mounted on the specimens' surface for monitoring purposes as shown in Figure 4a,b. The sensor type was wideband WD 100–900 kHz manufactured by PAC, Princeton, New Jersey (USA). The transducer was attached on the specimens' surface using a suitable glycerine based coupling agent. AE signal acquisition was performed via a four channel 16bit PCI/DSP-4 by PAC data acquisition system. Pre-amplification of 40 dB and band-pass filtering of 20–1200 kHz was performed using general purpose voltage preamplifiers with 0/20/40 dB variable gain (2/4/6-AST Auto Sensor Testing Preamplifiers by PAC). Five samples were tested for each type of material system and for each type of experiment.

2.6.2. Knock Down Effect and Healing Performance Assessment

As mentioned, the current study is structured in two main investigations. The first covers the assessment of the performance of composites by comparing and evaluating the properties of the reference material to the modified capsule-based composite system. The change in performance is commonly referred to as the knock-down effect. The second investigation deals with the self-healing efficiency of the modified composite. It is anticipated the recovery of the measured property up to a percentage once the composite is integrated with a healing functionality.

Mode II Experiments

In the case of MODE II tests, specimens were loaded up to the load drop point which coincided with the first acoustic emission signs. The knock down effect (KNE) was calculated as a percentage according to Equation (1).

Modified samples after load/reload followed the healing cycle of 48 h at 80 °C in a controlled oven. All samples were after left to cool down at room temperature. Experiments were conducted again at the same conditions after the healing process was completed. Healing efficiency (HE) regarding the modified material is presented as a ratio of the healed to the unhealed measured property and is based on Equation (3). At least five specimens were tested for each material.

$$KNE \% = \frac{\text{Reference Property} - \text{Modified Property}}{\text{Reference Property}} * 100 \quad (1)$$

$$HE \% = \frac{\text{Property AH}}{\text{Property BH}} * 100 \quad (2)$$

where AH is the measured property After Healing and BH the initial property Before Healing.

Three-Point Bending Experiments

Regarding the knock down effect the same protocol was followed for three-point bending experiments and measurements calculated according to Equation (3).

Concerning the self-healing assessment, it is taken into account that fiber breakage is a catastrophic type of failure for composites and capsules fail to be sufficient in such an extensive damage. Thus, it is recommended fiber breakage to be avoided and focus is given on matrix microcracking.

To this view, the first category of specimens either reference (R) with no capsules or modified (M) with capsules loaded up to fracture in order to obtain the materials properties. Subsequently, the second category of specimens subjected to unloading/reloading three-point bending conditions in order to induce in a controlled manner new damage within the composite. Loading was interrupted by one unload/reload cycle. The loading was terminated at the first acoustic emission activity (AE) indicating the presence on new matrix microcracking damage. Reloading up to fracture separated either to specimens before (BH) or after the healing cycle (AH) The objective is to measure the residual strength and modulus of each material when damage is induced during loading. Figure 5 depicts the flowchart of the loading conditions. At least five specimens were tested for each concept while reference samples were tested at their initial state (un-healed).

$$KNE \% = \frac{\text{Reference Property at Fracture} - \text{Modified Property at fracture}}{\text{Reference Property at fracture}} * 100 \quad (3)$$

$$HE \% = \frac{\text{Property AH reloading up to fracture} - \text{Property BH reloading up to fracture}}{\text{Property BH reloading up to fracture}} * 100 \quad (4)$$

where AH is the measured property after healing and BH the initial property before healing.

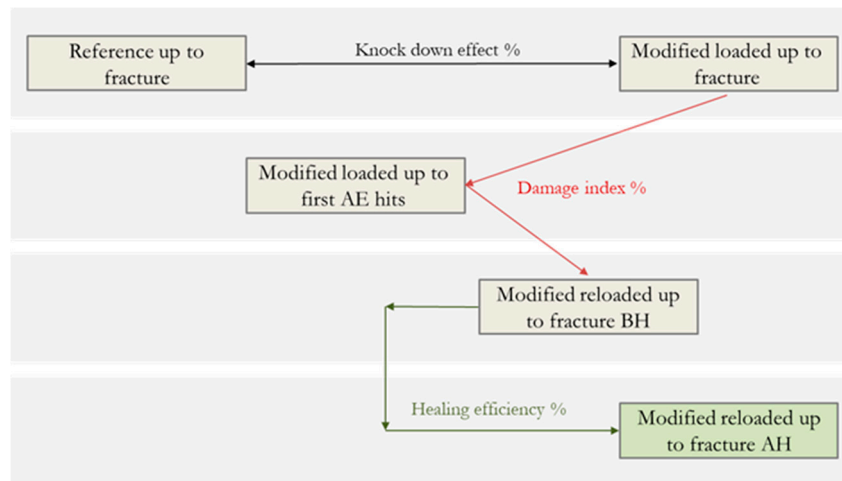


Figure 5. Flowchart for loading/reloading protocol for both reference and modified materials before and after healing.

The new damage index was measured for both reference and modified materials according to Equation (5).

$$\text{Damage Index \%} = \frac{\text{Property at fracture}}{\text{Property reloaded up to fracture}} * 100 \quad (5)$$

3. Results and Discussion

3.1. Scanning Electron Microscopy (SEM)

SEM images of the EPON 828/EPA-filled microcapsules obtained at two levels of magnification (i.e., $\times 30$ and $\times 65$) are depicted in Figure 6. As can be seen, the SEM photographs revealed that the capsules were spherical in shape and had rough exterior shell walls. It is evident that capsules tend to agglomerate after drying and sieving. This effect can be attributed to the low concentration of EMA surfactant [30]. In addition, the rough porous morphology of the outer surface results to an enhanced mechanical interlocking between the capsules and the host polymer matrix. This is a crucial parameter since the efficiency of a capsule-based self-healing system is highly affected by the capsules facture.

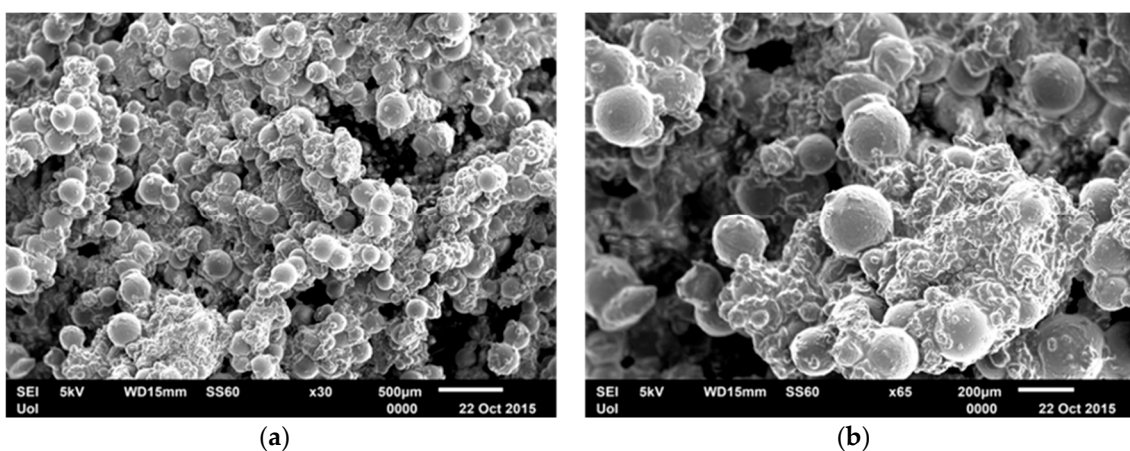


Figure 6. SEM images obtained at different levels of magnification, $\times 30$ (a) and $\times 65$ (b).

Capsule mean diameter was determined at 200 μm from data sets of at least 200 measurements while the standard deviation was calculated at 36 μm . Figure 7a depicts the dimensional analysis conducted using the SEM software while Figure 7b illustrates the microcapsules size distribution

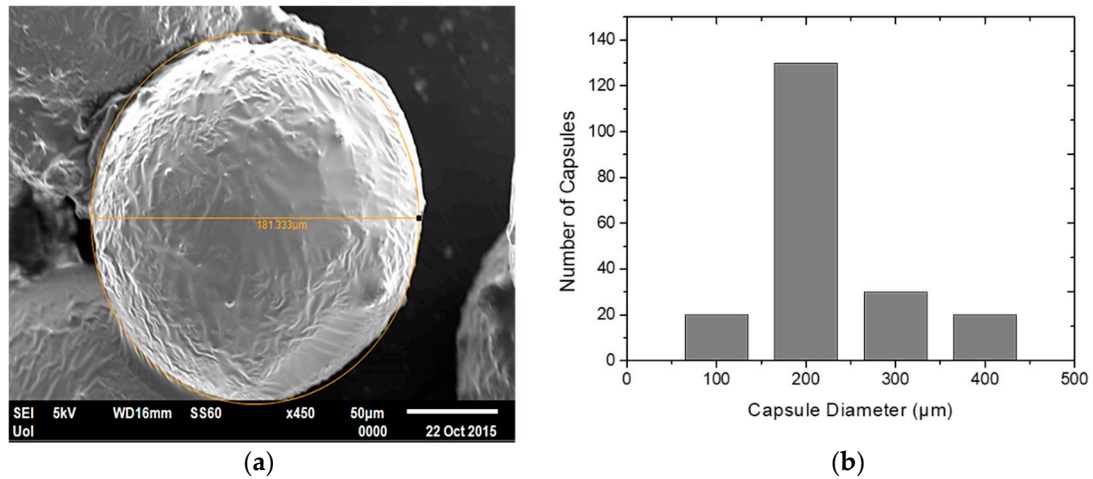


Figure 7. Microcapsules (a) Dimensional analysis and (b) size distribution.

3.2. Fracture Results

The Mode II fracture toughness values and the standard deviations of Carbon Fiber Reinforced Polymers (CFRPs) samples are presented in Figure 8a. The recovery of G_{IIC} and the typical behavior of a representative sample are depicted in Figure 8b. It is observed that the capsules integration led to a 14% decrease in the G_{IIC} compared to the reference material. Capsules are considered as voids which interrupt the integral structure of the composite. Furthermore, studies have revealed [31] that due to the fragile nature of the capsules, their contribution to the load bearing capability of epoxy is negligible, which can explain the observed reduction.

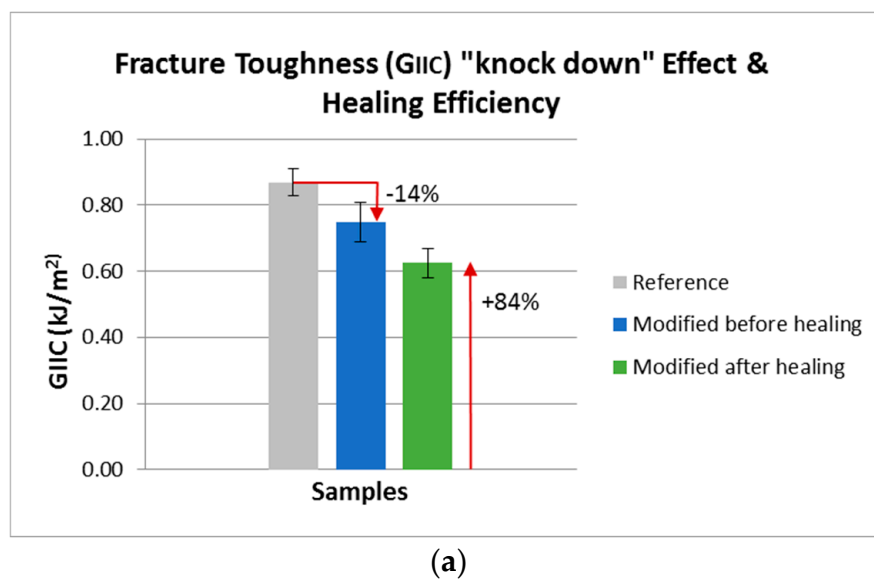


Figure 8. Cont.

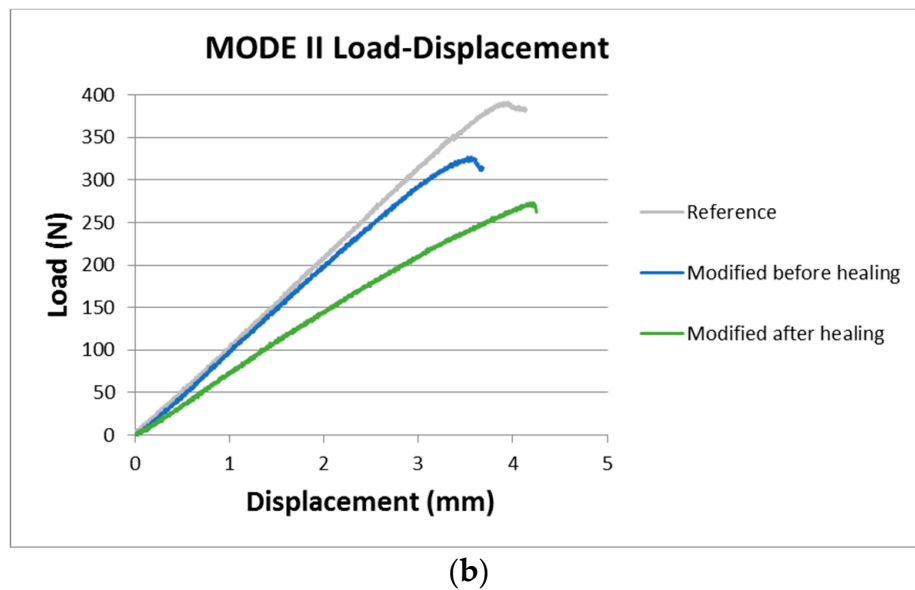


Figure 8. Mode II experiments main results for (a) knock down effect and healing efficiency regarding the fracture toughness (b) typical behavior of representative sample of reference, modified before and after healing.

As far as the self-healing efficiency is concerned, the recovery in G_{IIC} values reached 84% after the healing process compared to the modified samples. This significant recovery percentage is a clear indication of efficient interlocking between the capsules and the matrix material. Moreover, it can be attributable to the formation of a denser healed interlaminar region due to the polymerization of the healing system. In view of this, it is assumed that the selected low content of 10%wt. in combination with the highly active catalyst [18,32] resulted in a minor knock down effect and a high healing efficiency.

3.3. Three-Point Bending Results

The flexural strength and modulus were assessed regarding the knock down effect (Equation (3)) due to the capsule's integration and also for their recovery after the healing process (Equation (4)).

A decrease of up to 5% and 6% was measured for flexural strength and modulus, respectively, as shown in Figure 9a,b. Furthermore, the representative curve for a reference and a modified specimen is presented in Figure 9c. Several parameters have been reported as being responsible for the knock down factor (i.e., capsules size and content, method of incorporation etc., [33]), one of the most crucial is the dispersion of the capsules within the matrix material. Capsules were deliberately integrated at certain layers, as detailed described in section "2.3 Composite manufacturing", in order to reduce the knock down effect. It should be noted that the measured decrease is not considered crucial as the developed material can provide an additional functionality, that of self-healing.

The percentage of the damage index due to the unloading/reloading conditions was measured for the developed materials according to Equation (5). The induced damage index followed the same trend for both reference and modified material at each property. More precisely, for flexural strength (FS) 21% and 23%, and flexural modulus (FM) 23% and 25, respectively, to the reference and modified material as presented in Figure 10a. A representative diagram of load-extension for a modified specimen is presented in Figure 10b during loading/reloading conditions.

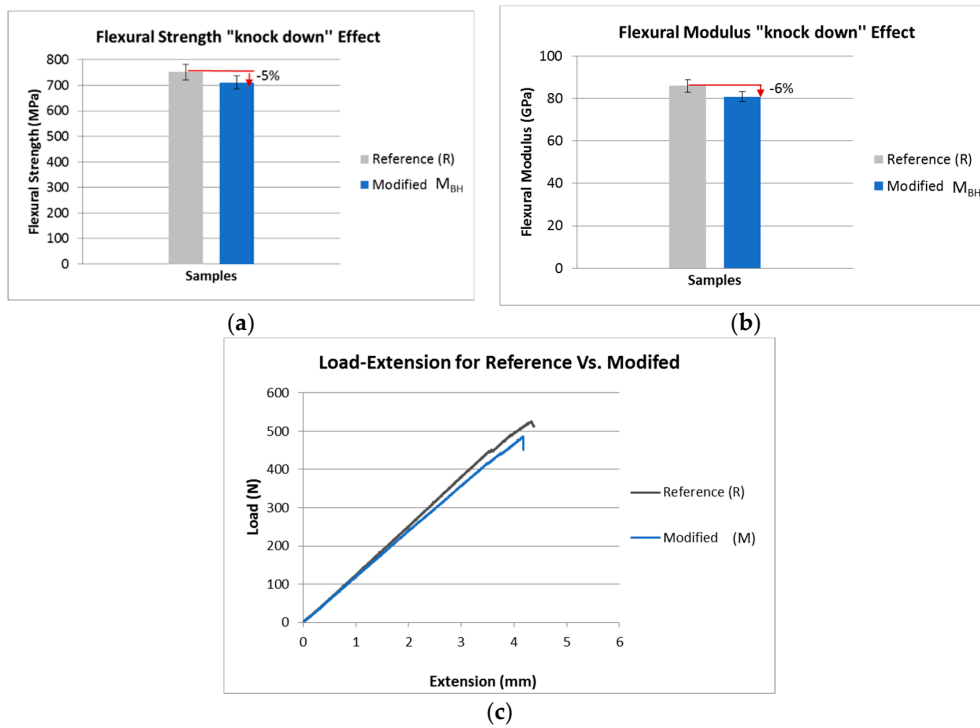


Figure 9. Knock down effect for (a) flexural strength, (b) flexural modulus and (c) representative curve of load-extension for reference and modified specimen up to fracture.

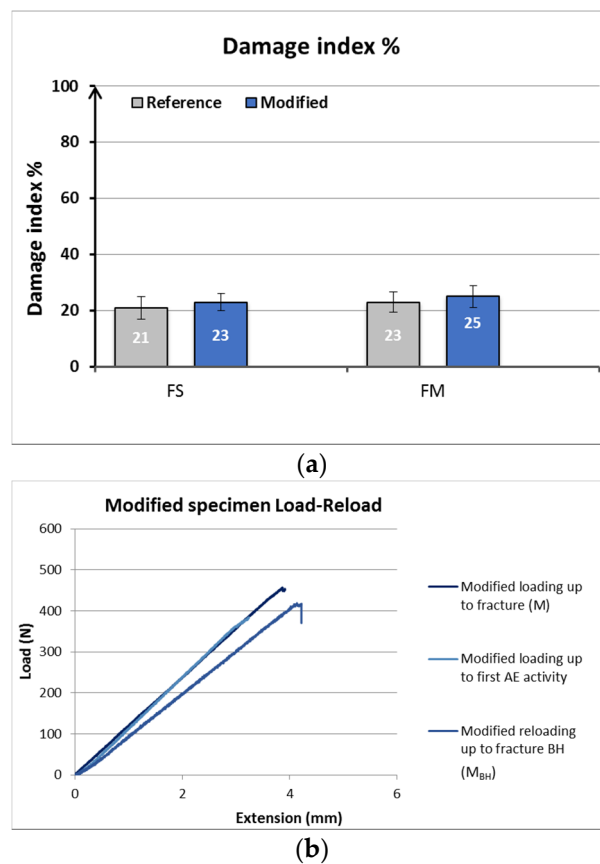


Figure 10. (a) Percentage of damage index during unloading/reloading protocol for flexural strength and flexural modulus. (b) Load-extension for modified specimen during loading/reloading conditions.

Once damage was quantified the healing efficiency was evaluated. In Figure 11a,b the average values of self-healing efficiency are observed. An additional comparison is mentioned that of the reference material when reloaded up to fracture after the damage index. The aim is to compare the after and before healing properties, not only with the modified material, but also with the reference with no healing functionality. A representative diagram from a specimen of each category is shown in Figure 11c comparing the reloading behavior of modified before, after healing and the reference.

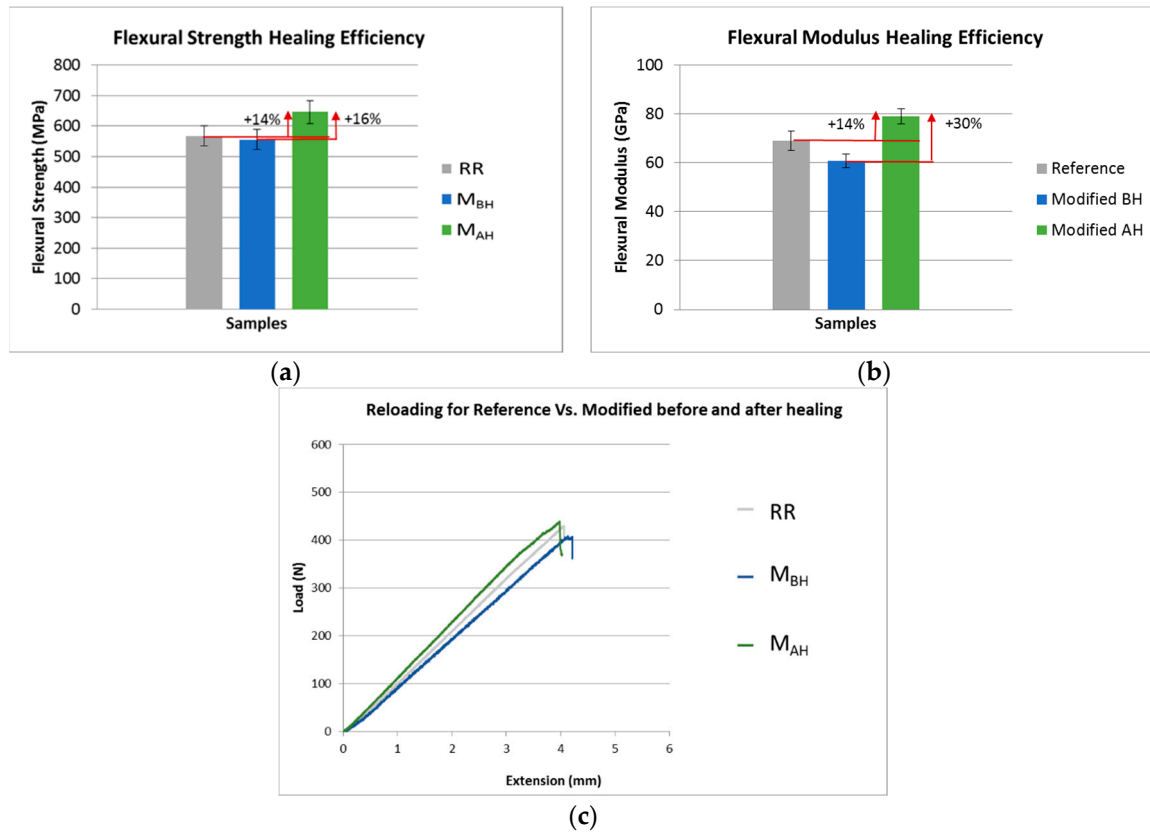


Figure 11. (a) Flexural Strength Healing Efficiency. (b) Flexural Modulus Healing Efficiency. (c) load-extension of reloading conditions for a reference specimen, modified before and after healing.

A proportion of 16% for flexural strength and 30% for flexural modulus was recovered after the healing process when compared to the unhealed modified material. The adhesion between the capsules and the matrix proved to be sufficient and compatible to provide recovery. It is worth mentioning that the modified material after the healing process performed better during reloading up to fracture even to the reference material at the same conditions. More precisely, both flexural strength and modulus were increased up to 14%. A representative diagram of a specimen at each category is shown in Figure 11c, comparing exclusively the reloading behavior of the modified before, after healing (M_{BH}, M_{AH}) and the reference (RR). Figure 12 summarizes all of the results for each concept and involves an explanatory schematic for each comparison. Table 1 provides the final outcomes for the behavior of the developed materials.

Loading Conditions	Average Flexural Strength (FS) (MPa)	Average Flexural Modulus (FM) (GPa)	Damage index FS (%)	Damage index FM (%)		
R	Reference up to fracture	752.50	86.00	21.00	23.00	Damage Index % Reference
	Reference loading up to first AE activity	-	85.77			
	Reference reloading up to fracture RR	567.82	69.07			
M	Modified up to fracture	711.02	80.88	23.00	25.00	Damage Index % Modified
	Modified loading up to first AE activity M _{BH}	-	76.02			
	Modified reloading up to fracture BH	556.47	60.79			
	Modified reloading up to fracture AH M _{AH}	645.98	79.00			

Knock down effect % (KNE) Healing Efficiency % (HE)

Figure 12. Unloading/Reloading protocol for three-point bending tests. Values and schematic of each measurement. Abbreviations: AE, Acoustic Emission; AH, after healing; BH, before healing.

Table 1. Main results for the knock down effect and the self-healing efficiency regarding the flexural strength and modulus of the tested materials.

Main Results	Flexural Strength (FS) (MPa)	Flexural Modulus (FM) (GPa)
KNE %: R vs. M	-5	-6
HE %: M _{AH} vs. M _{BH}	+16	+30
HE %: M _{AH} vs. RR	+14	+14

The supremacy of the material after the healing process confirms the successful activation and performance of capsules. Furthermore, the induced damage of the composite was limited only to matrix cracking which was perceived by the hits captured by the AE sensors. In case of fiber breakage, the capsules healing ability would have negligible effect on the fiber dominated failure.

3.4. Acoustic Emission Results

Recordings of AE during Mode II experiments are presented in Figure 13. Reference and modified specimens reported marginal differences in terms of the number of hits at maximum load. Capsules breakage recordings were most probably eliminated due to the relatively high selected threshold of 40 dB [27]. It is worth mentioning that the acoustic activity of the healed specimens was, as anticipated, slightly higher than those of the reference and unhealed ones. This could be attributed to the partially repaired damage and for this reason the acoustic emission activity started at an earlier stage, resulting in more overall AE hits.

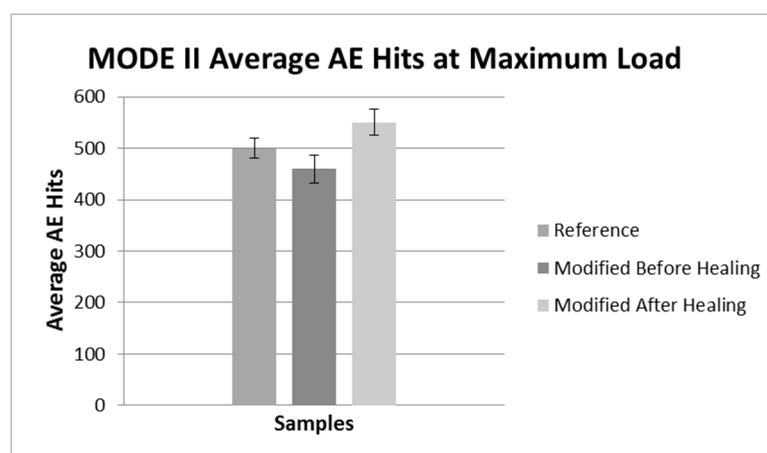


Figure 13. Average AE hits of Mode II experiments for all specimens.

In the case of 3PB experiments, one may hypothesize that the total recovery measured may indicate no new damage within the composite until the loading stops and thus, there is no new damaged area to be healed. To investigate this phenomenon and assess whether damage was indeed healed or not, the protocol of unloading/reloading was utilized in order to determine the felicity effect (FE) which refers to the presence of detectable/significant acoustic emission activity at a load level below the previous maximum applied. According to the literature [34], the difference at the load onset of emission is a reliable indicator of new damage to the FRP. As load increases and the material suffers more damage, the AE hits increase, and the FE becomes more pronounced. Furthermore, the Felicity Ratio (FR) was calculated based on Equation (6) [35]. It is described as the fraction of load at which the acoustic emission is recorded to the previous maximum applied load. A decreasing FR corresponds to a growing level of damage in the structure being monitored.

$$FR = \frac{\text{Load (F2) at onset of significant AE during reloading}}{\text{Load (F1) at onset of significant AE during loading}} < 1 \quad (6)$$

The onset of emission at an earlier load during reloading was confirmed and is shown in Figure 14. The presence of some level of damage, possibly at the level of matrix microcracks, which eventually triggers the embedded healing system is thus ensured with the aid of acoustic emission observations. Figure 14 depicts the felicity effect and a calculated FR of 0.95 for one representative modified specimen. In all tested samples the felicity ratio was less than one and this was used as a prerequisite for the validity of the above argumentation.

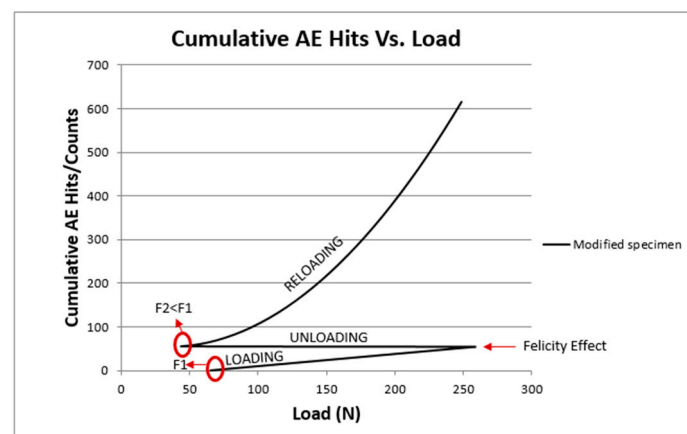


Figure 14. Cumulative AE hits vs. load for a representative modified specimen under 3PB conditions. Depiction of felicity effect and load values used for the calculation of felicity ratio.

4. Concluding Remarks

In this study, the mechanical properties of low-content capsule-based CFRPs were investigated. The investigation was focused at determining the influence of capsules integration within a composite by measuring the knock down effect. Furthermore, the self-healing efficiency of the developed materials was evaluated. The interlaminar fracture toughness (G_{IIC}) did not have a significant decrease (−14%) compared to the reference composite. Towards the same direction, flexural strength and modulus were slightly decreased, 5% and 6%, respectively, with regards to the neat material. As far as the self-healing efficiency is concerned, G_{IIC} recovered up to 84%. Flexural strength healing efficiency reached the 16% and 14% while flexural modulus 14% and 30% compared to the unhealed and the reference material, respectively.

It is worth mentioning that the assessment of healing presented in the current study, is with a couple of alternations to the standard protocol recommended by ASTM D7264/D6264M-07. In order to avoid the catastrophic failure of composites, which is the fiber breakage, an unloading and reloading

cycle was applied. This protocol is closer in real applications where loadings are not constant, and by no means fiber breakage is acceptable.

Furthermore, the self-healing functionality is supposed to be targeted in specific areas which are susceptible in damage. For this reason, UF capsules were not dispersed to all composite layers in the case of 3-point bending, which resulted in a notable healing efficiency by ensuring simultaneously a controlled and low knock down effect

The healing efficiency rates mostly demonstrate the good adhesion between the polymer matrix and the encapsulate healing system combined with the highly reactive character of the scandium triflate.

The acoustic emission recordings were utilized to support the experimental process by ensuring the damage mechanism of matrix microcracking.

It is conceivable that the low integrated content of capsules when combined with a proper catalyst can provide recovery without significantly compromising the initial mechanical performance. With further developments, the capsule-based composites have the potential for being incorporated into a variety of applications to provide the desired multifunctionality.

Author Contributions: Conceptualization, V.K., S.T. and A.P.; methodology, S.T., X.T. and D.B.; validation, S.T., V.K. and A.P.; formal analysis, M.K., X.T. and D.B.; investigation, M.K., X.T. and D.B.; resources, M.K., X.T. and D.B.; writing—original draft preparation, X.T., M.K. and D.G.B.; writing—review and editing, S.T.; visualization, X.T., M.K. and D.B.; supervision, V.K. and A.P.; project administration, V.K. and A.P.; funding acquisition, V.K. and A.P. All authors have read and agreed to the published version of the manuscript.

Funding: This research received no external funding.

Conflicts of Interest: The authors declare no conflict of interest.

References

- White, S.R.; Sottos, N.R.; Geubelle, P.H.; Moore, J.S.; Kessler, M.R.; Sriram, S.R. Autonomic healing of polymer composites. *Nature* **2001**, *409*, 794–797. [[CrossRef](#)] [[PubMed](#)]
- Blaiszik, B.J.; Kramer, S.L.; Olugebefola, S.C.; Moore, J.S.; Sottos, N.R.; White, S.R. Self-Healing Polymers and Composites. *Annu. Rev. Mater. Res.* **2010**, *40*, 179–211. [[CrossRef](#)]
- Bekas, G.D.; Baltzis, D.; Paipetis, A.S. Nano-reinforced polymeric healing agents for vascular self-repairing composites. *Mater. Des.* **2017**, *116*, 538–554. [[CrossRef](#)]
- Coope, T.S.; Wass, D.F.; Trask, R.S.; Bond, I.P. Repeated self-healing of microvascular carbon fibre reinforced polymer composites. *Smart Mater. Struct.* **2014**, *23*, 115002. [[CrossRef](#)]
- Kostopoulos, V.; Kotrotsos, A.; Baltopoulos, A.; Tsantzalidis, S.; Tsokanas, P.; Loutas, T.; Bosman, A.W. Mode II fracture toughening and healing of composites using supramolecular polymer interlayers. *Express Polym. Lett.* **2016**, *10*, 914–926. [[CrossRef](#)]
- Tsilimigkra, X.; Baltopoulos, A.; Tsantzalidis, S.; Kotrotsos, A.; Siakavellas, N.; Kostopoulos, V.; Flórez, S. Strategies on implementing a potential self-healing functionality in a composite structure. *Ciência Tecnologia dos Materiais* **2016**, *28*, 147–154. [[CrossRef](#)]
- Brown, E.N.; Sottos, N.R.; White, S.R. Fracture testing of a self-healing polymer composite. *Exp. Mech.* **2002**, *42*, 372–379. [[CrossRef](#)]
- Jones, A.S.; Rule, J.D.; Moore, J.S.; Sottos, N.R.; White, S.R. Life extension of self-healing polymers with rapidly growing fatigue cracks. *J. R. Soc. Interface* **2007**, *4*, 395–403. [[CrossRef](#)]
- Yuan, L.; Liang, G.; Xie, J.; Li, L.; Guo, J. Preparation and characterization of poly (urea-formaldehyde) microcapsules filled with epoxy resins. *Polymer* **2006**, *47*, 5338–5349. [[CrossRef](#)]
- Cosco, S.; Ambrogio, V.; Musto, P.; Carfagna, C. Urea-formaldehyde microcapsules containing an epoxy resin: Influence of reaction parameters on the encapsulation yield. *Macromol. Symp.* **2006**, *234*, 184–192. [[CrossRef](#)]
- Blaiszik, B.J.; Caruso, M.M.; McIlroy, D.A.; Moore, J.S.; White, S.R.; Sottos, N.R. Microcapsules filled with reactive solutions for self-healing materials. *Polymer* **2009**, *50*, 990–997. [[CrossRef](#)]
- Schwab, P.; Grubbs, R.H.; Ziller, J.W. Synthesis and applications of RuCl₂ (CHR')₂ (PR₃)₂: The influence of the alkylidene moiety on metathesis activity. *J. Am. Chem. Soc.* **1996**, *118*, 100–110. [[CrossRef](#)]
- Brown, E.N.; White, S.R.; Sottos, N.R. Retardation and repair of fatigue cracks in a microcapsule toughened epoxy composite—Part II: In situ self-healing. *Compos. Sci. Technol.* **2005**, *65*, 2474–2480. [[CrossRef](#)]

14. Moll, J.L.; White, S.R.; Sottos, N.R. A Self-sealing Fiber-reinforced Composite. *J. Compos. Mater.* **2010**, *44*, 2573–2585. [[CrossRef](#)]
15. Patel, A.J.; Sottos, N.R.; Wetzel, E.D.; White, S.R. Autonomic healing of low-velocity impact damage in fiber-reinforced composites. *Compos. Part A Appl. Sci. Manuf.* **2010**, *41*, 360–368. [[CrossRef](#)]
16. Sanada, K.; Yasuda, I.; Shindo, Y. Damage progression and notched strength recovery of fiber-reinforced polymers encompassing self-healing of interfacial debonding. *J. Compos. Mater.* **2015**, *49*, 1765–1776. [[CrossRef](#)]
17. Kessler, M.R.; Sottos, N.R.; White, S.R. Self-healing structural composite materials. *Compos. Part A Appl. Sci. Manuf.* **2003**, *34*, 743–753. [[CrossRef](#)]
18. Coope, T.S.; Mayer, U.F.; Wass, D.F.; Trask, R.S.; Bond, I.P. Self-healing of an Epoxy Resin Using Scandium (III) Triflate as a Catalytic Curing Agent. *Adv. Funct. Mater.* **2011**, *21*, 4624–4631. [[CrossRef](#)]
19. Rong, M.Z.; Zhang, M.Q.; Zhang, W. A novel self-healing epoxy system with microencapsulated epoxy and imidazole curing agent. *Adv. Compos. Lett.* **2007**, *16*, 167–172. [[CrossRef](#)]
20. Caruso, M.M.; Blaiszik, B.J.; White, S.R.; Sottos, N.R.; Moore, J.S. Full Recovery of Fracture Toughness Using a Nontoxic Solvent-Based Self-Healing System. *Adv. Funct. Mater.* **2008**, *18*, 1898–1904. [[CrossRef](#)]
21. Bekas, D.G.; Tsirka, K.; Baltzis, D.; Paipetis, A.S. Self-healing materials: A review of advances in materials, evaluation characterization and monitoring techniques. *Compos. Part B Eng.* **2016**, *87*, 92–119. [[CrossRef](#)]
22. Mallick, P.K. *Fiber-Reinforced Composites: Materials, Manufacturing, and Design*, Dekker Mechanical Engineering, 2nd ed.; CRC Press: New York, NY, USA, 1993.
23. Manfredi, E.; Cohades, A.; Richard, I.; Michaud, V. Assessment of solvent capsule-based healing for woven E-glass fibre-reinforced polymers. *Smart Mater. Struct.* **2015**, *24*, 015019. [[CrossRef](#)]
24. Yin, T.; Rong, M.Z.; Zhang, M.Q.; Yang, G.C. Self-healing epoxy composites—Preparation and effect of the healant consisting of microencapsulated epoxy and latent curing agent. *Compos. Sci. Technol.* **2007**, *67*, 201–212. [[CrossRef](#)]
25. Moll, J.L.; Jin, H.; Mangun, C.L.; White, S.R.; Sottos, N.R. Self-sealing of mechanical damage in a fully cured structural composite. *Compos. Sci. Technol.* **2013**, *79*, 15–20. [[CrossRef](#)]
26. Szebényi, G.; Czigány, T.; Vermes, B.; Ye, X.J.; Rong, M.Z.; Zhang, M.Q. Acoustic emission study of the TDCB test of microcapsules filled self-healing polymer. *Polym. Test.* **2016**, *54*, 134–138. [[CrossRef](#)]
27. Yadav, J.S.; Kumar, V.N.; Rao, R.S.; Priyadarshini, A.D.; Rao, P.P.; Reddy, B.V.S.; Nagaiah, K. Sc (OTf) 3 catalyzed highly rapid and efficient synthesis of β -enamino compounds under solvent-free conditions. *J. Mol. Cat. A Chem.* **2006**, *256*, 234–237. [[CrossRef](#)]
28. Zhu, Y.; Rong, M.Z.; Zhang, M.Q. Self-healing polymeric materials based on microencapsulated healing agents: From design to preparation. *Prog. Polym. Sci.* **2015**, *49*, 175–220. [[CrossRef](#)]
29. Brown, E.N.; Kessler, M.R.; Sottos, N.R.; White, S.R. In situ poly(urea-formaldehyde) microencapsulation of dicyclopentadiene. *J. Microencapsul.* **2003**, *20*, 719–730. [[CrossRef](#)]
30. Blaiszik, B.J.; Sottos, N.R.; White, S.R. Nanocapsules for self-healing materials. *Compos. Sci. Technol.* **2008**, *68*, 978–986. [[CrossRef](#)]
31. Keller, M.W.; Sottos, N.R. Mechanical Properties of Microcapsules Used in a Self-Healing Polymer. *Exp. Mech.* **2006**, *46*, 725–733. [[CrossRef](#)]
32. Coope, T.S.; Wass, D.F.; Trask, R.S.; Bond, I.P. Metal Triflates as Catalytic Curing Agents in Self-Healing Fibre Reinforced Polymer Composite Materials. *Macromol. Mater. Eng.* **2014**, *299*, 208–218. [[CrossRef](#)]
33. Tagliavia, G.; Porfiri, M.; Gupta, N. Analysis of flexural properties of hollow-particle filled composites. *Compos. Part B Eng.* **2010**, *41*, 86–93. [[CrossRef](#)]
34. Fowler, T.J. Acoustic Emission Testing of Fiber Reinforced Plastics. *J. Tech. Counc. ASCE* **1979**, *105*, 281–289.
35. Abraham, A.R.A.; Johnson, K.L.; Nichols, C.T.; Saulsberry, R.L.; Waller, J.M. *Use of Statistical Analysis of Acoustic Emission Data on Carbon-Epoxy COPV Materials-of-Construction for Enhanced Felicity Ratio Onset Determination*; NASA-JSC White Sands Test Facility: Las Cruces, NM, USA, 2012; Volume 3, pp. 154–196.

